Engineering Journal of the University of Qatar, Vol. 14, 2001, pp. 105 – 125

FINITE ELEMENT ANALYSIS OF TUBULAR INDUCTION ACCELERATORS

J. H. H. Alwash,
M A. Al-Maayouf, and L. J. Qasir,
Electrical Engineering Department
College of Engineering
University of Baghdad
Baghdad , Iraq

ABSTRACT

The paper develops a method of analyzing tubular induction accelerators based on the finite element technique. The method takes end effects (due to current discontinuities at the rotor edges) into consideration. The performance is predicted for both air and iron cored tubular accelerators. A manipulation is given to reduce computation time which gives acceptable results.

NOMENCLATURE

Ac .....9-component of magnetic vector potential at the centroid of a triangular element, wb/m
B_r, B_θ, B_z.....r, θ and z-component of magnetic flux density vector, T
e.....superscript referring to the element
F_r, F_θ, F_z.....r, θ and z-component of force vector, N
I.....rms value of phase current, A
K.....wave length factor, rad/m
K_w.....fundamental winding factor w
L_c.....coil width, m c
Nc.....number of turns per coil c
q.....number of slots per pole per phase
r_c.....r-coordinate of the centroid of a triangular element, m
Sd.....slot depth, m
μ.....permeability, H/m
σ.....rotor conductivity, mho/m
τ.....pole pitch, m
ω.....angular velocity, rad/s

χ.....functional, function of a function
{F}.....column vector to account for stator current
[N] .....shape function
[ ].....matrix notation
{ }.....column vector notation
Re{ }.....real part of quantity in brackets
*.....complex conjugate

1. INTRODUCTION

A tubular induction accelerator is composed of one tubular motor or more, where each motor is considered as individual stage such that acceleration is achieved in a single or multistage. The tubular motor is of the long stator-short rotor variant.

The stator accelerated travelling field can have more than one synchronous speed where each synchronous speed of the travelling field represents an individual stage. The advantage of accelerated field is to reduce the heating losses produced in the rotor, thus increasing the efficiency[1]. In a previous paper[2], an optimized design of accelerator is presented for minimum stator length based on the conventional circuit. Driga and Weldon[3] presented a modified version of the equivalent circuit of the air-cored accelerators of the short rotor variant. Analysis of air cored tubular accelerators is also developed[4] using the coupled circuit method.

It is the object of this paper to present a two dimensional finite element technique which is adequate to study the performance of low acceleration rate tubular accelerators. As a second object, a mathematical technique to reduce the computational time is also presented.

2. MATHEMATICAL MODEL

The accelerated travelling field may be achieved by one of three methods:

i. Varying the pole pitch of the stator (VPP).
ii. Varying the frequency of the stator current (Vf).
iii. Varying the pole pitch and the frequency of the stator (Vf-VPP).

Variable pole pitch (VPP) can be achieved by using constant number of slots per pole per phase with a graded winding which is fabricated by increasing the coil spacing and turns. Also VPP can be achieved by increasing number of slots per pole per phase.

The model chosen for the analysis consists of five sections (each section comprised 12 coil as in table (1)).

Table (1): Machine details (one section)

Number of poles	4
Number of slots (coils)	12
Slots per pole per phase	1
Stator length, mm	360
Outer stator core diameter (including tooth), mm	132
Inner stator core diameter, mm	32
Slot depth, mm	30
Slot width, mm	10
Slot pitch, mm	30
Pole pitch, mm	90
Number of turns per coil (slot)	175
Stator current, amp	5
Size of stator conductor	SWG 19
Frequency, Hz	50, 150, 250
Air gap length, m	4
Outer rotor diameter, mm	24
Inner rotor diameter, mm	18
Rotor conductivity, S/m	3.5×10^7
Rotor length, mm	90
Relative permeability of iron	2000

In the case of VPP, the original pole pitch is doubled in the second stage while the frequency is doubled in case of Vf. In the case of Vf-VPP, the frequency and pole pitch are doubled in the second stage.

The rotor is a hollow cylinder of pure aluminum filled with iron rods (for iron cored rotor) with one pole pitch length. The performance is predicted using the homogeneous media representation for stator excitation. The distribution of the fundamental component of the current density wave is given by:

$$J = J_m \exp[j(wt - kz)]$$

Where J_m is the peak primary current density and is given by[5]:

$$J_m = \frac{6}{\pi}\frac{\sqrt{2}N_c I}{L_c S_d}k_w \quad A/m^2$$

Where

$$k_w = \sin\frac{\Pi L_c}{2\tau}\sum_{n=1}^{q}\sin\left[\frac{2n+2q-1}{6q}\right]\pi$$

Therefore the current density varies as $e^{-jk_1 z}$ for the first stage and as $e^{-jk_2 z}$ for the second stage where

$$k_1 = \frac{\pi}{\tau_1}$$

$$k_2 = \frac{\pi}{\tau_2}$$

and $\tau_1 < \tau_2$

At the point where the two adjacent stages are attached to each other, there must be a continuity of the current density wave. This can be ensured by using even number of poles as shown in Fig. 1. The solution is based on the following assumptions:

1. The stator current is known everywhere and has only one component which is in the azimuthal director.

2. All state variables vary sinusiodally with time at power frequencies so that displacement current are negligible.
3. The conductivity of iron for stator and rotor is neglected and the working condition of the field is at the linear region of B-H curve.
4. All field components decay to zero at sufficiently far radial distances from machine axis.
5. The rotor joule heating is negligible at the operating velocities[1].
6. Friction force between stator and rotor is neglected.

The analysis of a machine in which a short rotor is accelerating very rapidly is a complex problem[2] due to the following effects:

Edge Effects

The longitudinal edge effects arise from the discontinuity at the rotor edges. This effect is taken implicitly into consideration in the finite element solution.

Rapid Acceleration of the Rotor

The slip change was found in this case to be not more than 2.5% in a time t_1, which is the primary time constant.

In such a case[2] the static and dynamic force-speed curves will be identical.

Transient Associated with Switching on the Supply

The predicted performance of an accelerator is only likely to be seriously affected if the total travel time is sufficiently short compared with t which is the secondary time constant.

For the present analysis, in which the total time is long due to low acceleration rate, this effect can be neglected.

Rotor acceleration

Rotor acceleration is analyzed by following the motion of the rotor through the various stages. The work done in moving the rotor a distance (step size) $z_s = z_1 - z_0$ (Fig. 2) is given by:

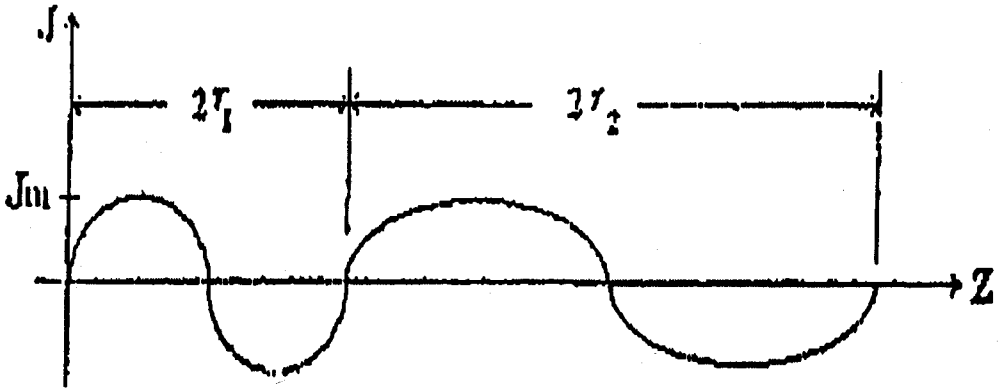

Fig. 1. Stator current density wave of a two-stage accelerator

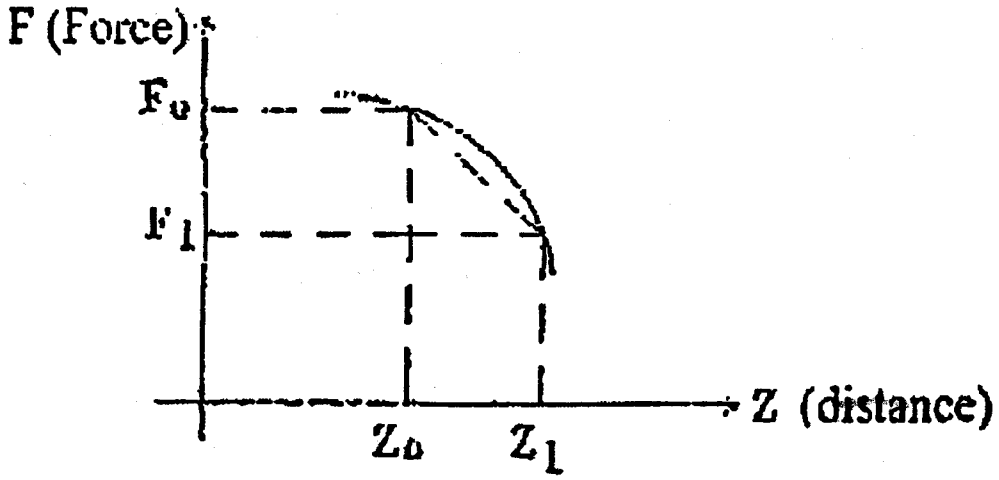

Fig. 2. Evaluation of new rotor speed at new position

$$w = \frac{1}{2}(F_0 + F_1)Z_s \qquad (1)$$

Which is developed as a kinetic energy in the rotor and is given by:

$$w = \frac{1}{2}m(v_1^2 + v_0^2) \qquad (2)$$

Combining equation (1) and (2) gives:

$$v_1^2 = v_0^2 + \frac{Z_s}{m}(F_0' + F_1)$$

where:

v_0 = Initial rotor velocity at initial position of rotor center z_0
v_1 = New rotor velocity at new rotor position z_1
F_0 = Force applied on the rotor moving at v_0
F_1 = Force applied on the rotor moving at v_1
m = Mass of the rotor

In the foregoing analysis the acceleration is assumed constant through the infinitesimal rotor step size as the force hence:

$$v_1^2 = v_0^2 + \frac{2F_0}{m} Z_s \tag{3}$$

The validity of the above assumption depends on the step size of rotor advance. To account for the joule heating in the rotor for a step Z_s, we have:

$$W_s = \int_{v_0}^{v_1} s F v_s \, dt = \frac{1}{2} m[2v_s(v_1 - v_0) - (v_1^2 - v_0^2)] = mC_p \Delta t \tag{4}$$

Where v_s is the synchronous speed of the stage through which the rotor is moving, C_p is the specific heat and Δt is the temperature rise. From this equation the new rotor temperature can be found hence a new rotor conductivity may be used for the next rotor step.

To account for the effect of friction, the acceleration force become:

$$F = F_z - F_r = m\,a$$

Where F_r is the friction force which is mass and velocity dependent, i.e.,

$$F_r = f(m, v) = k_1 + k_2 v^{k_3}$$

k_1, k_2 and k_3 are found experimentally[4], therefore Eq. (3) becomes:

$$v_1^2 = v_0^2 + \frac{2Z_s}{m}(F_{z0} - F_{r0})$$

For the next rotor step v is considered as v, new F, F_{r0} are found then new rotor velocity can be obtained.

3. THE FINITE ELEMENT FORMULATION

The governing differential equation in cylindrical coordinates for the entire domain obtained from Maxwell's equation becomes:

$$\frac{\partial}{\partial r}\left(\frac{1}{\mu}\frac{1}{r}\frac{\partial}{\partial r}rA\right)+\frac{\partial}{\partial z}\left(\frac{1}{r}\frac{\partial A}{\partial Z}\right)=-J \tag{5}$$

The variational method implies formulating the above equation in terms of variational expressions called energy functional which coincide with the energy stored in the field[6]. The Euler equation of this functional will generally coincide with the original differential equation. For the present analysis the required functional reduces to:

$$\chi=\frac{1}{2}\int_R\int\frac{1}{\mu}\left[\left(\frac{\partial A}{\partial r}\right)^2+\left(\frac{\partial A}{\partial Z}\right)^2+\frac{2A}{r}\frac{\partial A}{\partial r}+\frac{A^2}{r^2}\right]r\,dr\,dz-\int_R\int A\,J\,r\,dr\,dz$$

where J represents either the impressed current density in the primary winding region or induced eddy current density in the secondary which is given by:

$$J=-jw\sigma A-\sigma V_z\frac{\partial A}{\partial Z}$$

and in non-conducting J = 0.

Fig. 3 shows the domain for finite element solution which employs two stage variable pole pitch accelerator. The overall domain is discretized using first order triangular elements where the variational functional is formulated in terms of nodal vector potential. The vector potential within each element is defined in terms of interpolation function and the vector potential at the three vertices, hence within each element, the magnetic vector potential is given by:

$$A^e(r,z)=\sum N_i(r,z)A_i=N_iA_i+N_jA_j+N_kA_k$$

The minimization functional χ gives the nodal potentials which are the same in the solution of the corresponding Euler equation. Therefore χ must be differentiated with respect to each nodal value which gives a set of equations whose number is equal to the number of nodes, i.e.,

$$\frac{\partial \chi}{\partial A_i} = 0 \quad \text{Leading to:}$$

$$[S]\{A\}+[T]\{A\} = \{F\} \tag{6}$$

where

- [S] is real and symmetric square matrix
- [T] is complex and asymmetric square matrix due to induced current in the rotor, being zero elsewhere.
- {A} is the overall vector potential column of the entire domain
- {F} is the corresponding force vector of the stator current density, being zero elsewhere

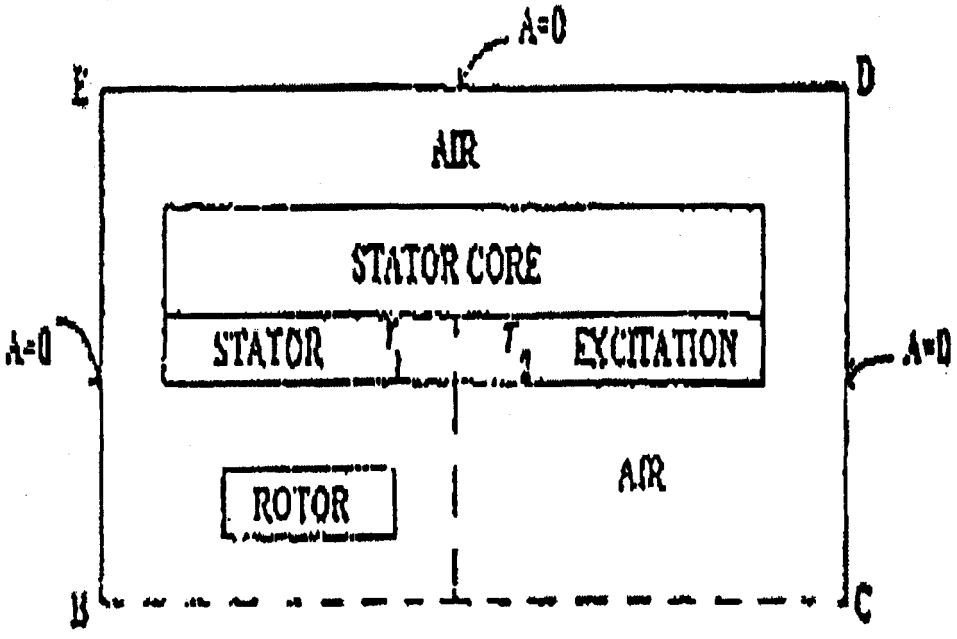

Fig. 3. Boundary definition of a two-stage accelerator of variable pole pitch

4. SOLUTION OF THE NON-LINEAR EQUATION

Eq. (6) is solved using the successive over-relaxation technique. The relaxation factor used in this work is optimized during iteration[7], i.e. each iteration has its own factor till the optimal value is obtained to minimize the number of iterations and execution time. Also the element size is optimized to give acceptable power mismatch.
The convergence of solution is obtained when the following inequality is satisfied:

$$\left\|\{\Delta A\}^i\right\|_\infty \leq \varepsilon$$

where $\left\|\{\Delta A\}^i\right\|_\infty$ is the maximum absolute value of the complex correction among all nodal values of the array vector $\{A\}$ at the i^{th} iteration, ε is the tolerance for solution convergence.

Automatic mesh generation subroutine is written to divide the domain into regions, the programs written can therefore be easily modified to study the performance of flat linear machines. It was found that a mesh size of 8% pole pitch in the axial direction is acceptable in the regions of the stator winding, the air gap and the rotor conductor. Outside these regions the mesh is made gradually coarse.

5. PERFORMANCE CALCULATION

Once the magnetic vector potential distribution in the overall domain is obtained the accelerating force which is in the axial direction may be calculated from J*B on the stator for a short rotor acceleration. Therefore for each element in the stator winding region:

$$F_z^e = \pi r_c \, \Delta \, \text{Real}\left\{J^e B_r^{e^*}\right.$$

For air cored rotor the concept of J*B on the rotor for short rotor acceleration can also be used. The overall propulsion force is obtained by summing up the contributions of individual forces then:

$$F_z = \sum_e F_z^e$$

It should be noted that the axial flux density B_z component in each element is given by:

$$B_z = \frac{\partial A}{\partial R} + \frac{A_c}{r_c}$$

where A_c is the magnetic vector potential at the centroid of the element whereas the normal flux density component B_r is given by:

$$B_r = -\frac{\partial A}{\partial Z}$$

6. COMPUTER IMPLEMENTATION

The step size for rotor center advance that can be chosen is related to rotor length or pole pitch whichever is the smaller. For the present analysis, a step size of 20% of the least pole pitch (which equals rotor length) is found to be acceptable. The step size for rotor center position should be made small enough in the regions between every two adjacent stages (where pole pitch varies abruptly), i.e., finer than that required to move the rotor along each stage (5% of pole pitch). This is due to the possible abrupt change in the rotor acceleration. However, when there is a continuous change in pole pitch then the acceleration will change smoothly and no such refinment is required. Table (2) gives comparison between three value of rotor step for single stage acceleration for the machine whose details are given in Table (1) using finite element technique, initial rotor velocity = 0, initial rotor center position from entry end of the accelerator is 90 mm and final rotor center position is 270 mm. The rotor is air cored.

The comparison shows that a mesh size of 10% of pole pitch and rotor step of 20% of pole pitch are quite acceptable in the sense that the three cases considered differ by less than 1%.

Table (2)

Mesh size in % of pole pitch	Rotor step in % of pole pitch	Final velocity (m/s)	Total elapsed time (sec)	Final acceleration (m/s^2)
5	5	1.2337	0.2849	4.0667
10	10	1.2327	0.285	4.0262
10	20	1.2345	0.2844	1.0194

7. COMPUTATIONAL AND TEST RESULTS

The finite element technique thus introduced required long computation time (essentially when the length of the accelerator is increased) due to increase in the number of nodes, therefore some form of manipulation has been devised to economize the computation time.

Constant Force-Axial Distance Characteristic

For single stage accelerator, the axial force on the rotor moving at a fixed velocity is constant and independent of rotor position within the stator. This is so since J*B on the stator side is constant for a given excitation irrespective of rotor position within the stator, which gives constant force distribution along approximately the entire length of the accelerator. Fig. 4 shows the propulsion force at standstill and 50 Hz frequency for iron cored rotor against axial distance (various rotor positions) which gives constant force distribution along approximately the entire length of the accelerator.

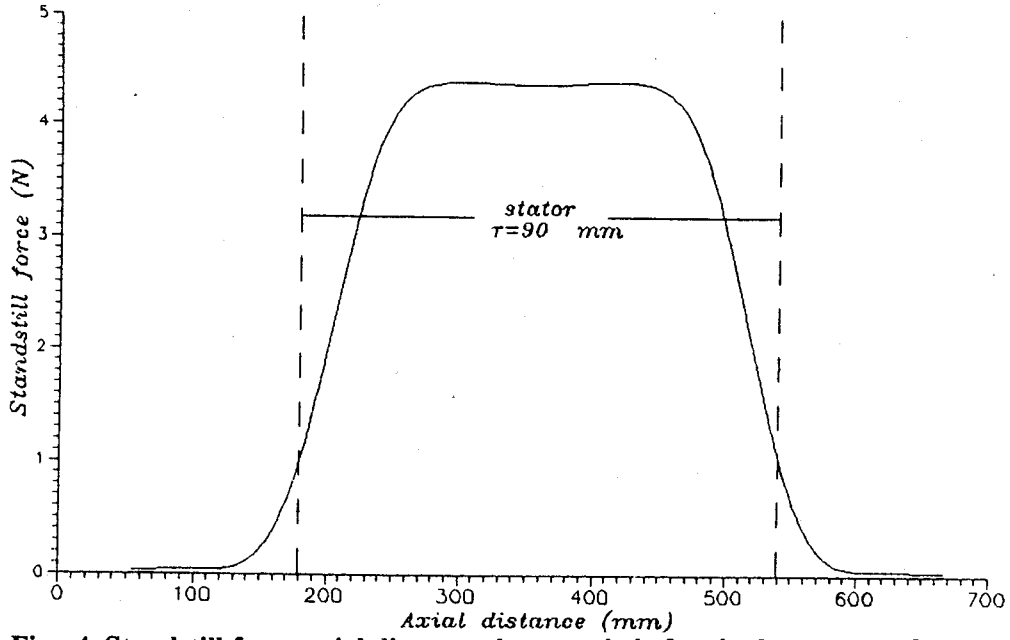

Fig. 4. Standstill force-axial distance characteristic for single stage accelerator at 50 Hz (iron cored rotor)

For multistage accelerator, the force on the rotor moving at fixed velocity is constant within each stage. Since the winding excitation is the same for each stage, the stages are considered as machines connected in series with the stage having no rotor being considered open circuited therefore, the only contribution to force comes from J*B on the stator of the stage containing the rotor. Fig. 5 shows the standstill force at 50Hz frequency for iron cored rotor against axial distance for two stages accelerator. It shows that for abrupt change in pole pitch there is a region between the two adjacent stage 9of width equal to one rotor) in which the force at standstill varies continuously due to mutual end effects of the two stages. For such case the rotor step is made finer (5% of pole pitch) to account for local change in constant force, however, for continuous change in pole pitch, no refinement is required.

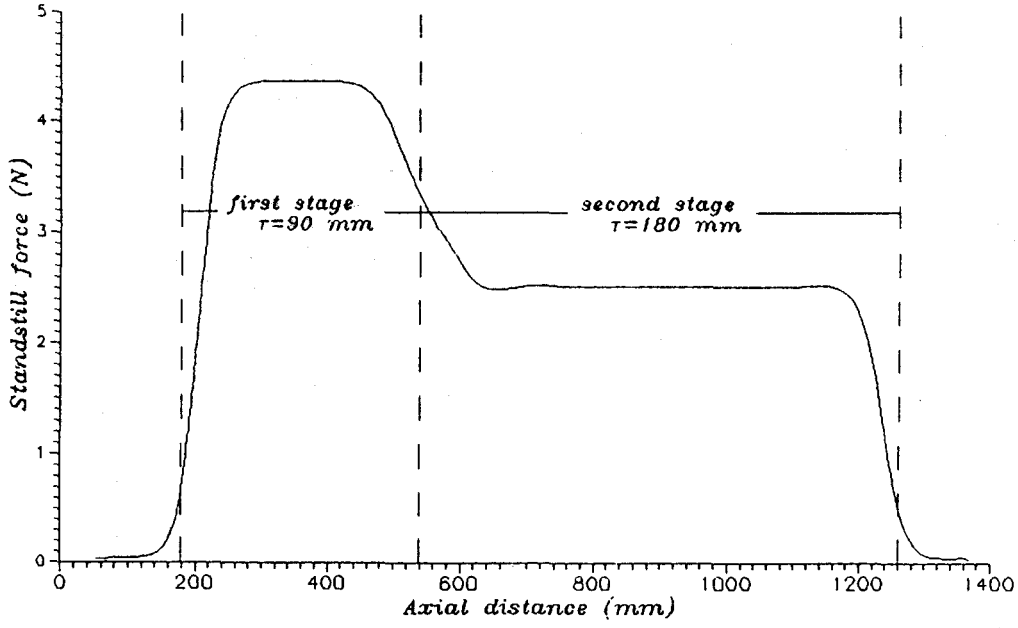

Fig. 5. Standstill force-axial distance characteristic for two-stage accelerator at 50 Hz (iron cored rotor)

Cubic Spline Interpolation

Fig. 6 shows the propulsion force-speed for iron cored short rotor machine whose dimensions are given in table (1), at three different frequencies. Each curve may be fitted through cubic spline interpolation and is used to follow the rotor motion through each stage depending on constant force-axial distance

characteristic, using the principle of rotor acceleration mentioned earlier. When the rotor enters each stage, the corresponding force-speed characteristic is used. It can be shown from Fig. 4 that when the rotor center is at one pole pitch from either end of the accelerator, the force changes linearly and rapidly. This can be manipulated in the cubic spline algorithm by using a force distance straight line fit such that the force on the rotor whose speed is increasing, is taken as a proportion of the constant force-axial distance characteristic while rotor step is made finer. However, if the rotor center is located at one pole pitch from the entry end, this manipulation can be discarded. Moreover, near the exit end, the rotor speed attains synchronous speed which means very small acceleration and speed increases linearly such that it can be extrapolated for the remaining pole pitch. Fig 7 shows a comparison between the finite element and cubic spline interpolation algorithms for a two-stage accelerator of variable frequency. The accelerator is single stage composed of 8-poles. The rotor center is located at z=90 mm from the entry end (which is zero on the curve) at standstill velocity. As the rotor center passes through the center of the accelerator, the frequency is changed from 60 Hz to 100 Hz using 3-phase sinusoidal supply to study the abrupt change in frequency in air cored rotor. The figure shows an excellent degree of compatibility through the entire distance between the two algorithms of less than 1%.

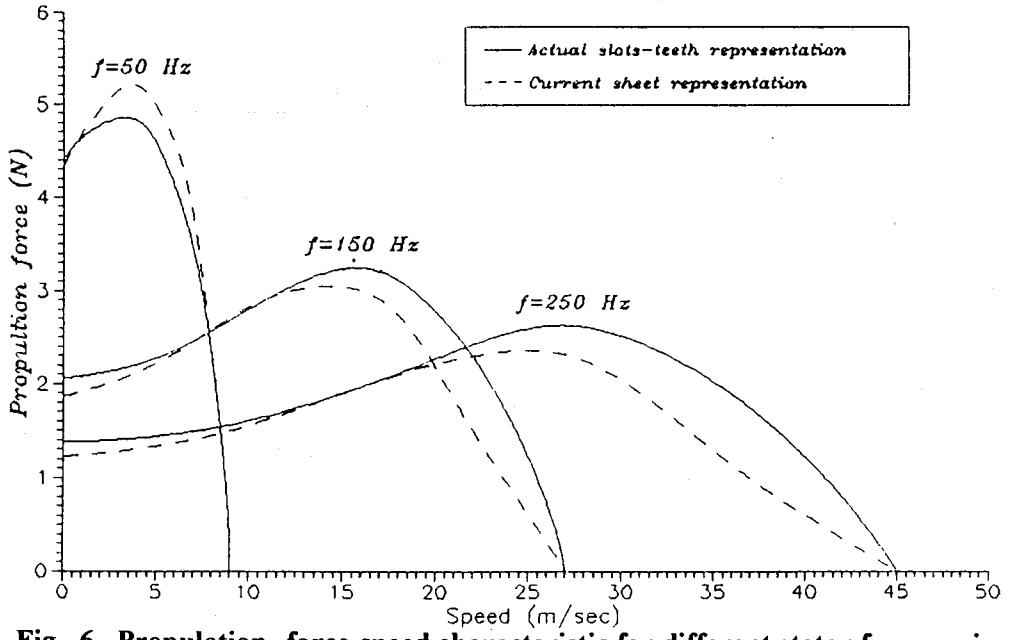

Fig. 6. Propulsion force-speed characteristic for different stator frequencies (iron cored rotor)

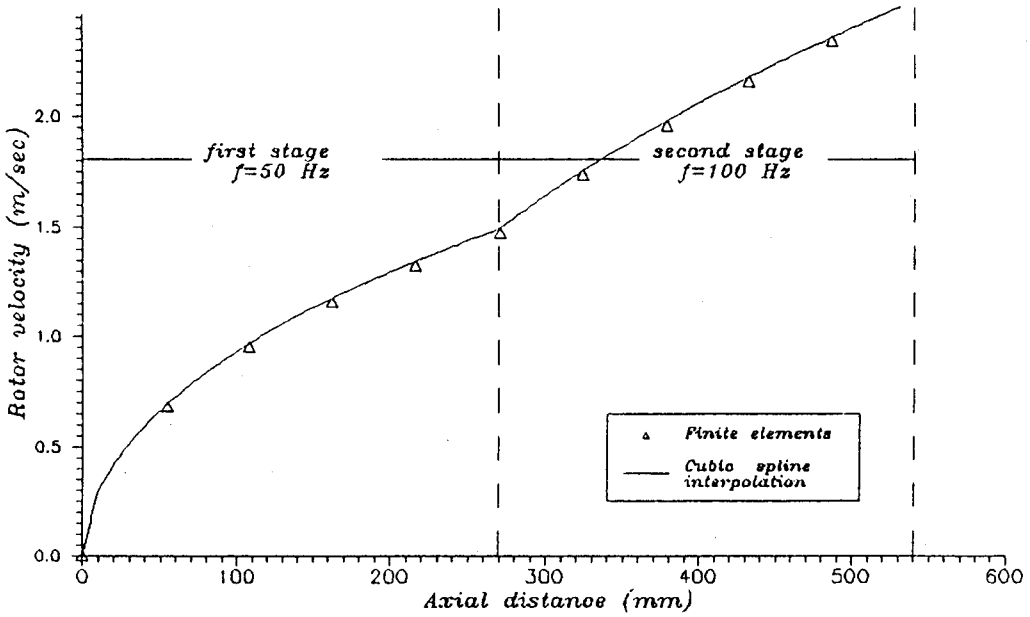

Fig. 7. Rotor velocity axial distance characteristic for two-stage accelerator of variable frequency (air-cored rotor)

An experimental model (single stage) is constructed to partially verify theoretical results. The tests were conducted at three different frequencies 50, 150 and 250 Hz at phase current of 2 Amps. Fig. (8-10) show the flux density component at the axis of symmetry (discrete winding representation) for standstill operation. Fig. (11) gives the standstill force against frequency showing the suitability of the finite element method. It is projected to construct an accelerator model which consists of five sections (each section comprises 12 coils) for each stage of the two stage accelerator to study the performance of the three types of acceleration. In the case of VPP, the second stage pole pitch is 180 mm while in the vase of Vf, the frequency is changed to 100 Hz when the rotor passes midway within the accelerator.

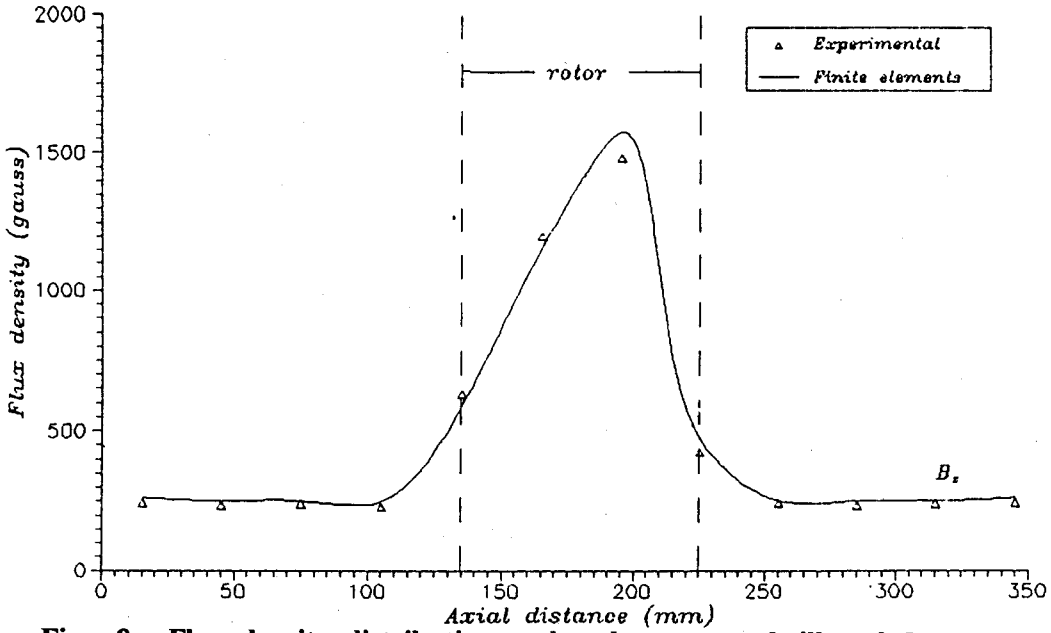

Fig. 8a. Flux density distribution under slots at standstill and frequency of 50 Hz

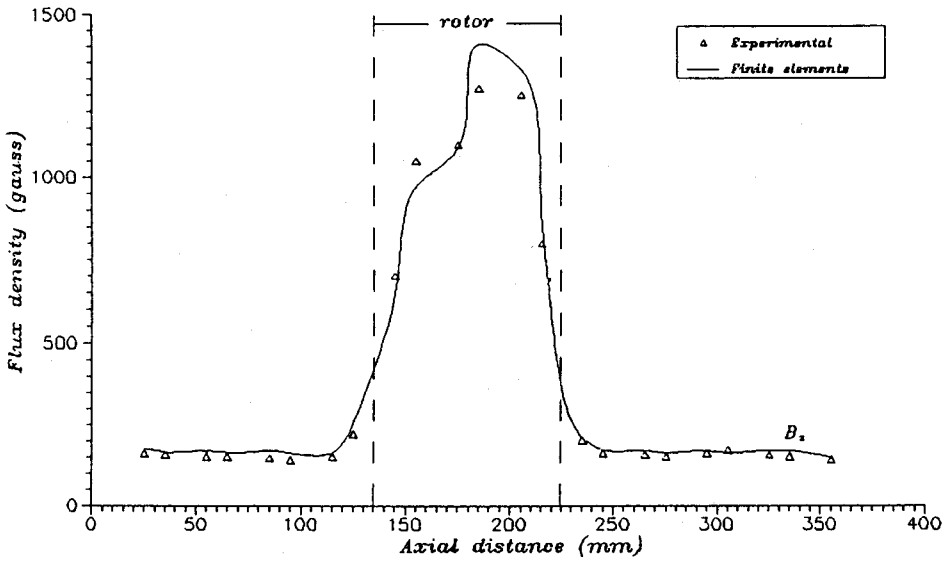

Fig. 8b. Flux density distribution under teeth at standstill and frequency of 50 Hz

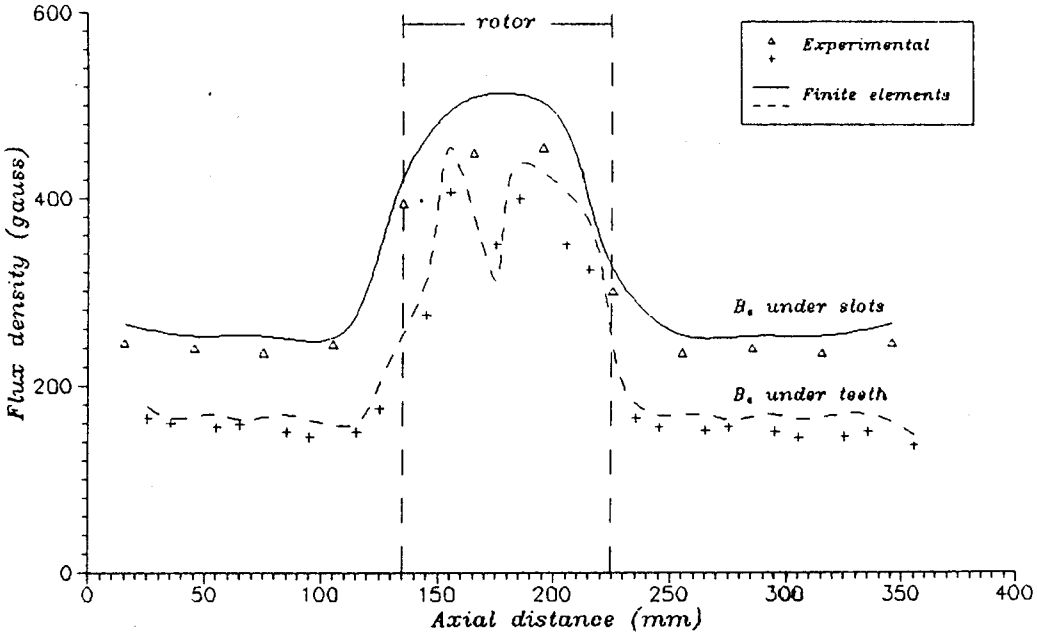

Fig. 9. Flux density distribution at standstill and frequency of 150 Hz

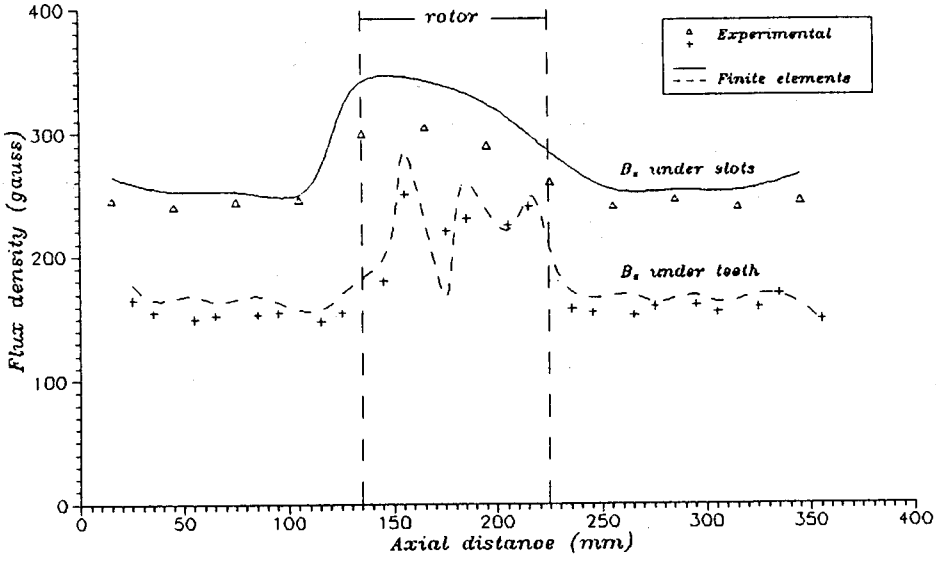

Fig. 10. Flux density distribution at standstill and frequency of 250 Hz

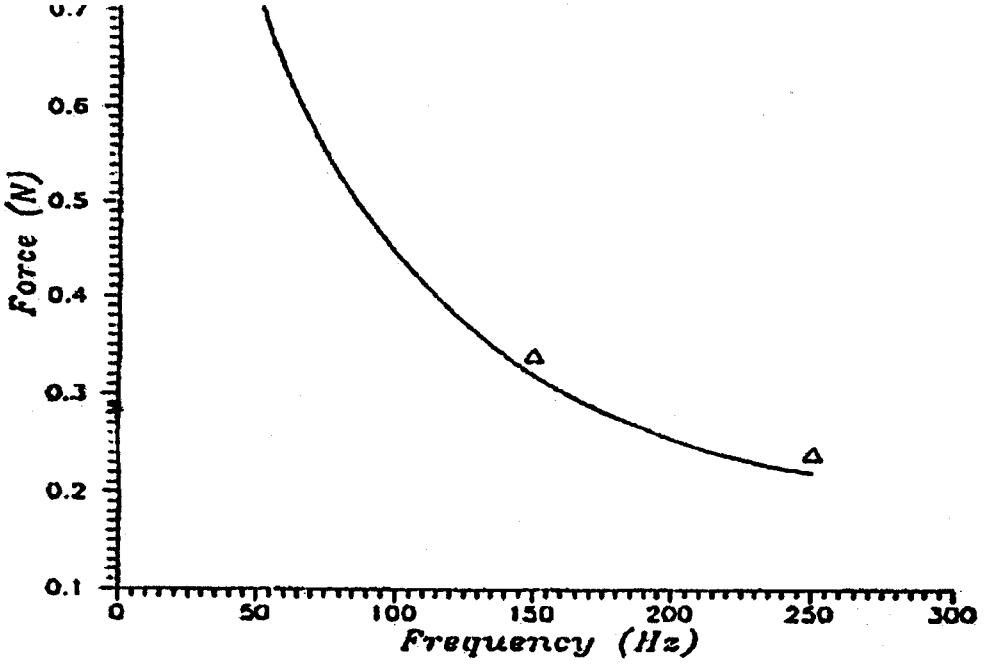

Fig. 11. Standstill propulsion force against frequency

Figs. (12-15) show the velocity and acceleration characteristics for air cored and iron cored rotor respectively for the three types of acceleration. Again the rotor center is located at one pole pitch from the entry end. The experimental two-stage accelerator model would be constructed to constitute the basis for future work.

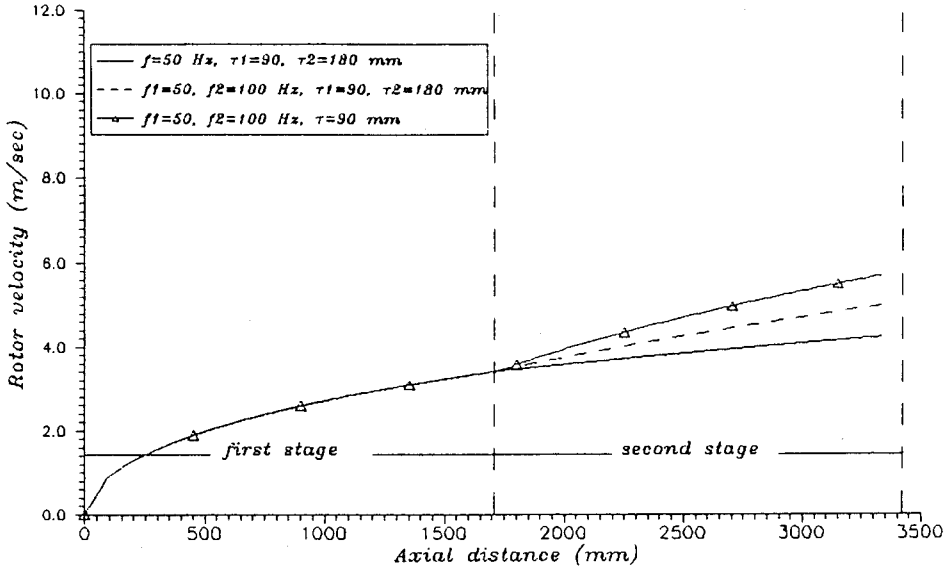

Fig. 12. Rotor velocity-axial distance characteristic for three types of two-stage acceleration (air-cored rotor)

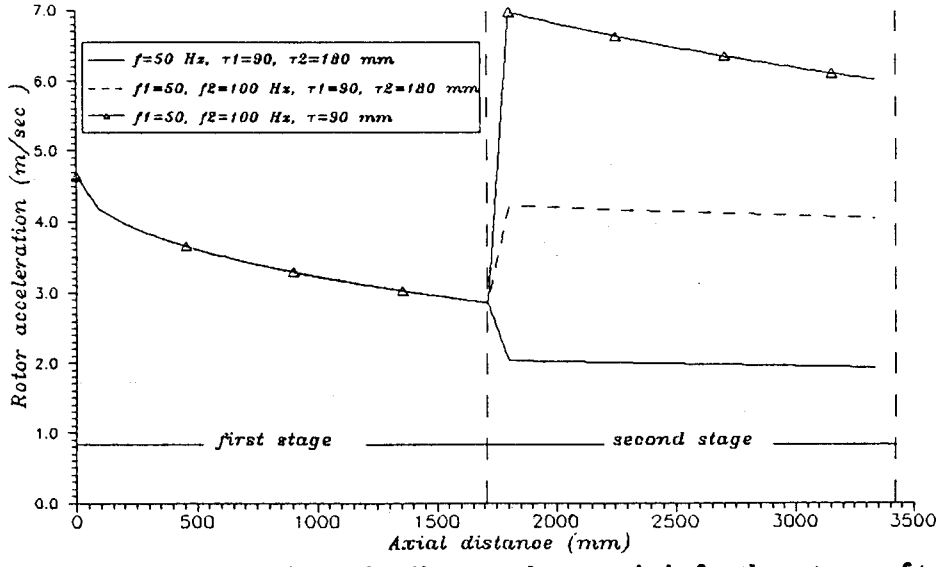

Fig. 13. Rotor acceleration-axial distance characteristic for three types of two-stage acceleration (air-cored rotor)

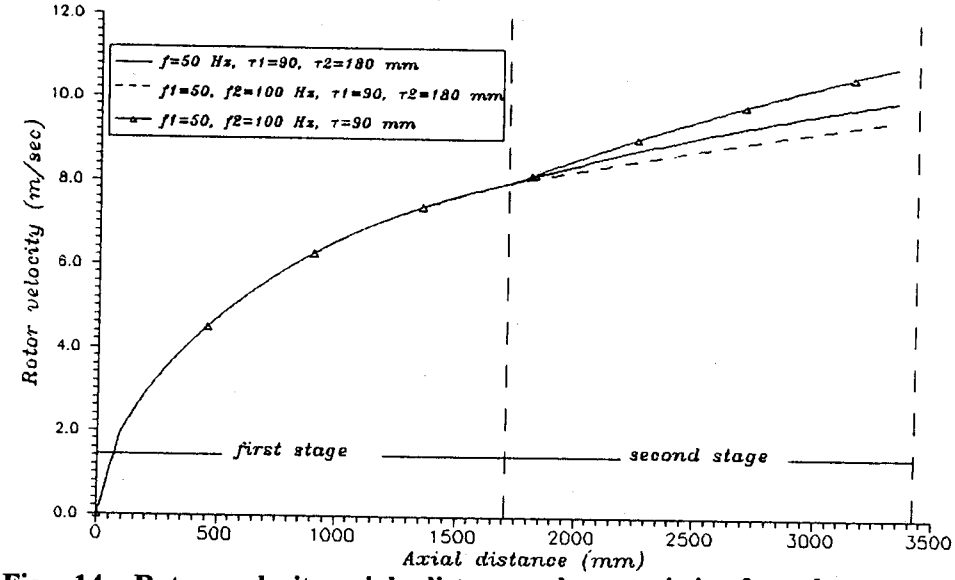

Fig. 14. Rotor velocity-axial distance characteristic for three types of two-stage acceleration (iron-cored rotor)

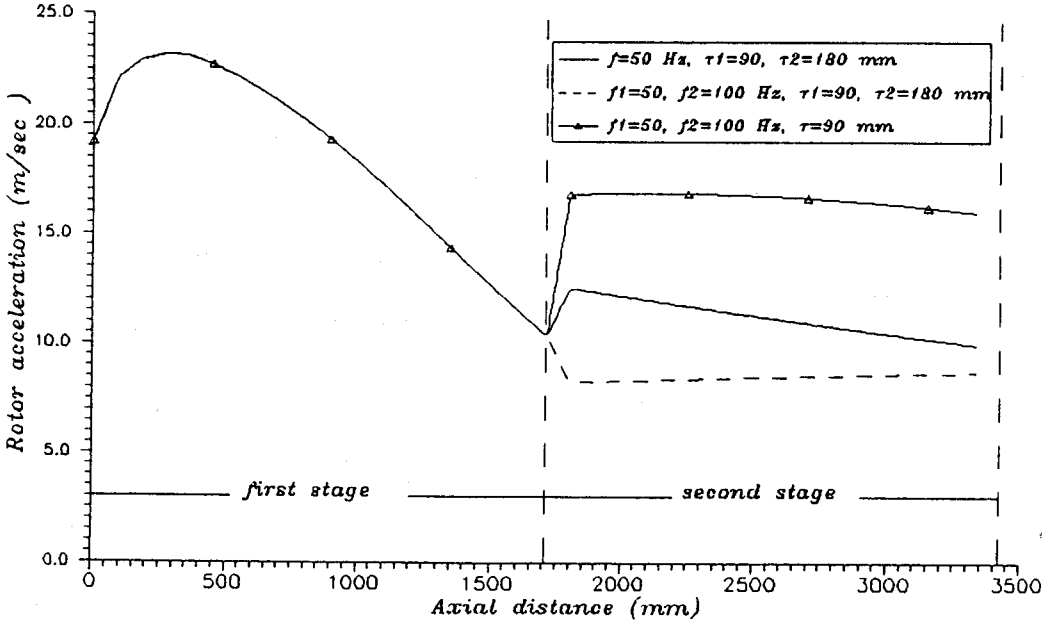

Fig. 15. Rotor acceleration-axial distance characteristic for three types of two-stage acceleration (iron-cored rotor)

8. CONCLUSION

In this study the finite element analysis of tubular induction accelerators is presented. The technique takes into account the actual configuration of the system which is absent in the conventional equivalent circuit method therefore, end effect are implicitly adopted. Friction force and rotor ohmic losses (which cause heating) can be easily taken into consideration. To simplify the analysis and save computation time, a manipulation is adopted which uses the force-speed characteristic for each stage in the analysis. The two techniques give high degree of compatibility.

REFERENCES

1. **Laithchwaite, E. R., 1966,** "Introduction Machines for special purposes", London: Newnes.

2. **Onuki, T.** and **Laithchwaite, E. R., 1971,** "Optimized design of linear induction motor accelerators", Proc. IEE, Vol. 118, pp. 49-355.

3. **Driga, M. D.** and **Weldon, W. F., 1989,** "Induction launchers design considerations", IEE Trans. On magnetics, Vol. 25, No. I, pp. 153-158.

4. **Williamson, S.** and **Leonard, P. J., 1986,** "Analysis of air cored tubular induction motors", Proc. IEEE, Vol., 133, Part B, No. 4, pp. 205-290.

5. **Al-Maayoof, M. A., 1981,** "A Study of linear induction motor using alternative models", Ph. D. Thesis. The City University, London, UK.
6. **Chari, M. V. K.** and **Silvester, P. P., 1980,** "Finite elements in electrical and magnetic field problems", New York, John Wiely and Sons.

7. **Qasir, L. J. B., 1993,** "Study of electromagnetic accelerator performance", M. Sc. Thesis, College of Engineering, University of Baghdad, Baghdad, Iraq.